

# PIV study for the analysis of planar jets in cross-flow at low Reynolds number

Vincenti I., Guj G., Camussi R., Giulietti E.

*University “Roma TRE”, Department of Ingegneria Meccanica e Industriale (DIMI), Via della Vasca Navale 79, 00146, Rome (Italy).*

**Keywords:** PIV, flow visualizations, jets in cross-flow, planar jet, stability.

## Abstract

An experimental investigation of the flow dynamics of planar jets in cross-flow is presented. Flow visualizations and Particle Image Velocimetry (PIV) measurements are performed at low jet Reynolds numbers ( $Re_j=5\div 200$ ) in a vertical water tunnel for jet-to-cross-stream velocity ratios  $R$  ranging from 0.5 to 12. The main point focused in the present work is the interaction between the shear-layer vortices (SLV) and the counter rotating vortex pair (CRVP) at different  $R$ . In order to clarify instability mechanisms, a planar jet with aspect ratio 50 issuing in the cross stream is considered. The PIV vector fields and flow visualizations are analysed to characterize the effect of  $R$  on the formation and evolution of large-scale vortices. Different behaviours are observed and the establishment of the different regimes is interpreted physically as an effect of the ratio  $R$  and of the jet Reynolds number which play an essential role on the destabilization mechanisms which lead to the formation of the jet shear-layer structures.

## List of symbols

$B$  = width of the duct of planar jet (mm)  
 $d$  = height of the duct of planar jet (mm)  
 $D$  = side of the square test section (mm)  
 $f$  = frequency (Hz)  
 $L$  = length of the duct of planar jet (mm)  
 $Q$  = mass flow rate (l/h)  
 $R$  = jet-to-cross stream velocity ratio  
 $U$  = velocity (cm/s)

### Subscripts

$j$  = jet  
 $\infty$  = referred to main flow (cross-stream)  
 $s$  = spatial

### Superscripts

\* = displacement

### Greek symbols

$\delta$  = boundary layer thickness (cm);  
 $\nu$  = kinematic viscosity of water at ambient temperature ( $m^2/s$ );  
 $\sigma$  = standard deviation (cm/s).

# 1. Introduction

The study of jets exhausting in cross-flows is an important aspect for many physical problems and applications in engineering and environmental aspects. Injectors for cooling systems and smoke exhaust from refineries, are two examples among many. In particular, the study and characterization of coherent structures which develop inside the cross-flow in the near and far field (with reference to the position of the exhausting orifice of the transverse jet) is an issue of great importance e.g. in the study of the interactions with the wall (important for flow control problems) and for the analysis of temperature distribution in low Prandtl number fluids (e.g. for thermal fatigue problems). Even if several works have been recently devoted to this subject (see e.g. [1]), further studies are needed in view of the complexity of the phenomenon. One of the basic aspects which needs clarifications, is the mutual influence and interference among different large scale vortical structures which develop when the jet is bent under the effect of the cross stream. Specifically, as observed for a circular jet in a cross-flow, the so called *Counter Rotating Vortex Pair* (CRVP) and the *Ring-Like Vortices* (RLV) determine the dominant features of the velocity and vorticity fields and their dynamic is of great interest from the practical viewpoint since they are mainly responsible for mixing, and for mass, momentum and heat transfer.

In the present work we focus attention on such vortex systems and on their reciprocal influence. CRVP and RLV vorticity always coexist and their interactions give rise to quite complicated behaviours that are not yet completely understood mainly for what concerns the instability mechanisms and the transition to a turbulent state.

According to Camussi, Guj and Stella [2] the destabilization of a circular jet in a low flow regime ( $R < 3$ ), driving the formation of the RLV structures, is associated with oscillations of the jet axis and it is delayed for increasing  $R$ . The instability mechanism which leads to the formation of the RLV seems therefore to be dominated by the jet axis curvature combined with the pairing of the CRVP, being the  $Re_j$  too low to induce on the jet shear layer any instability of Kelvin-Helmoltz type. In this sense, in the low  $R$  regime, the RLV usually observed by the visualization might be considered as a product of the CRVP destabilization.

In order to separate the instability mechanisms leading to the formation of the RLV with respect to the dynamics of the CRVP, a planar jet issuing in the cross stream has been considered. In this case the contribution of the CRVP is minimized thus the instability mechanisms are dominated by the RLV dynamics. In the case of a planar jet the term of RLV is changed with SLV (Shear Layer Vortices) because the vortical structures have not a shape like a ring. The study of the planar jet has been conducted at low Reynolds number  $Re_j = U_{jet} d_j / \nu$ .

The main point focused in the present work is the study of the mechanism of formation of SLV without CRVP at different jet-to-cross stream velocity ratio  $R = U_j / U_\infty$  (where  $U_j$  and  $U_\infty$  represent respectively the jet and cross-stream velocity). We wish to stress that the understanding of the instability mechanisms leading to a turbulent state is of practical interest to develop flow control strategies aimed, as an example, at anticipating the transition to turbulence and increase mixing.

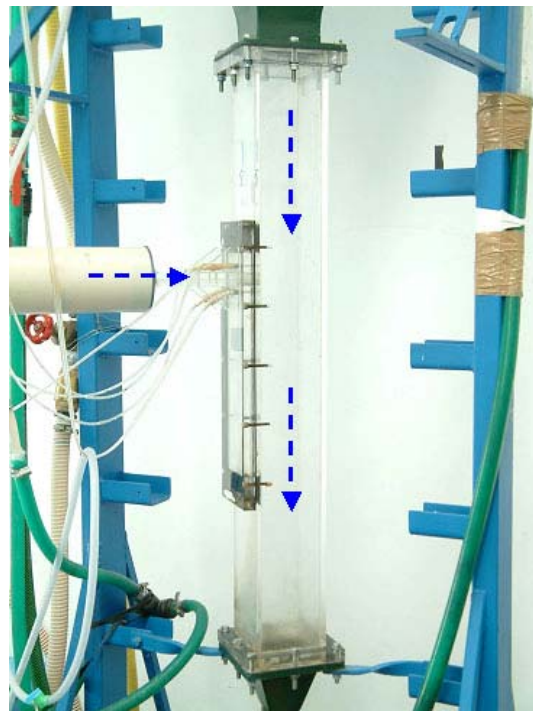
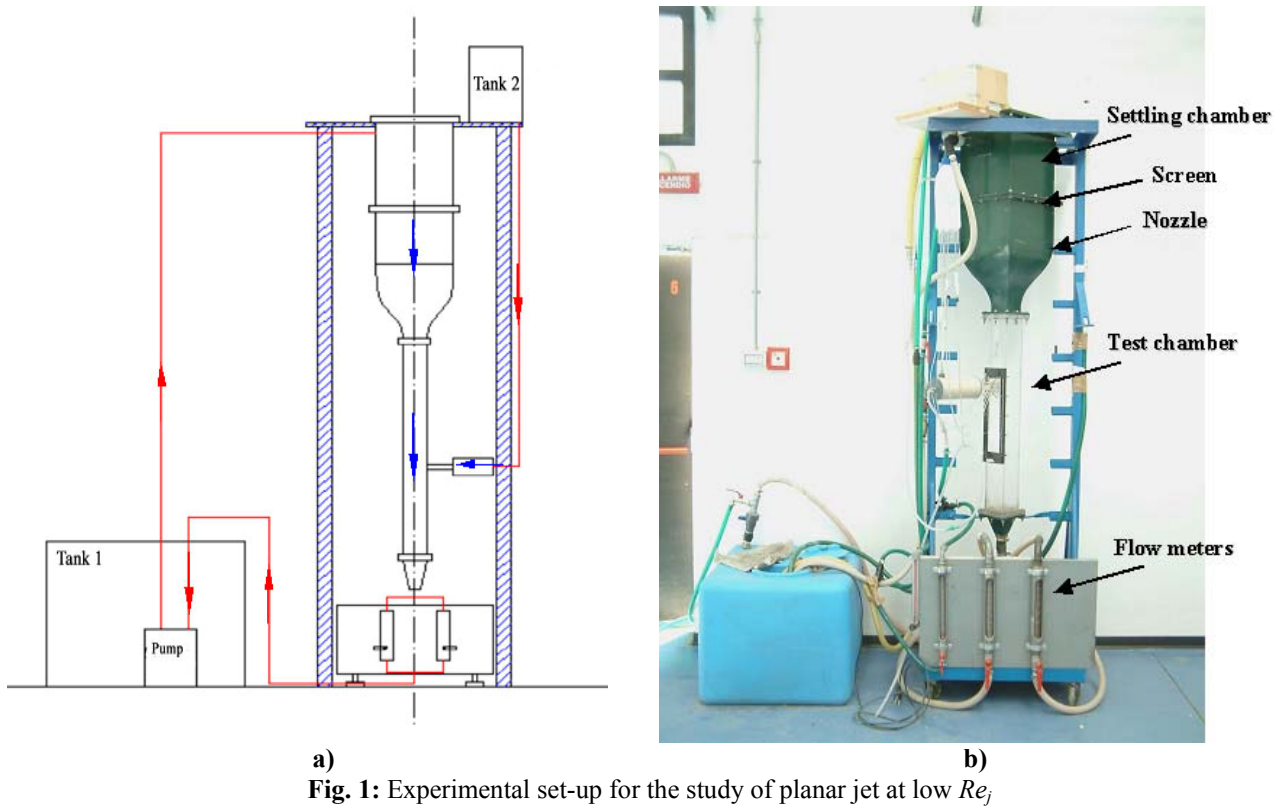
It should be stressed that the case of a cold planar jet issuing in a cross flow has been poorly studied in literature (see [3]) thus an ad hoc experiment has been designed and the experimental flow analysis is carried on through flow visualizations and PIV measurements.

## 2. Experimental set-up

The scheme of the experimental set up adopted in the study of the planar jet in the cross flow configuration is presented in Fig. 1.

The experimental analysis is performed in a gravity-driven water tunnel available at the fluid dynamic laboratory of the Department of Mechanics of the University "Roma TRE".

The settling chamber, equipped with honeycomb and screens, is followed by a contraction, with a ratio of 10, which accelerates the water flow into the square test section (Fig. 2). The mean velocities of the main flow and of the jet flow are exactly metered by flow meters.



The jet exit geometry (Fig. 3) was properly designed to achieve a large aspect ratio in order for a quasi-2D flow to be achieved at the jet exit ([4] and [5]). Indeed, the vertical opening is  $d=1\text{mm}$

large while the transverse width  $B$  is 50mm. Also the axial length (along the  $x$  direction) of the jet duct is ( $L=200\text{mm}$ ) quite larger than the vertical opening thus the jet exit flow is fully developed. The cross-water jet with 2D section is flush mounted in the middle of the test section (Fig. 2), perpendicular to the wall and it is gravity driven by an independent tank.

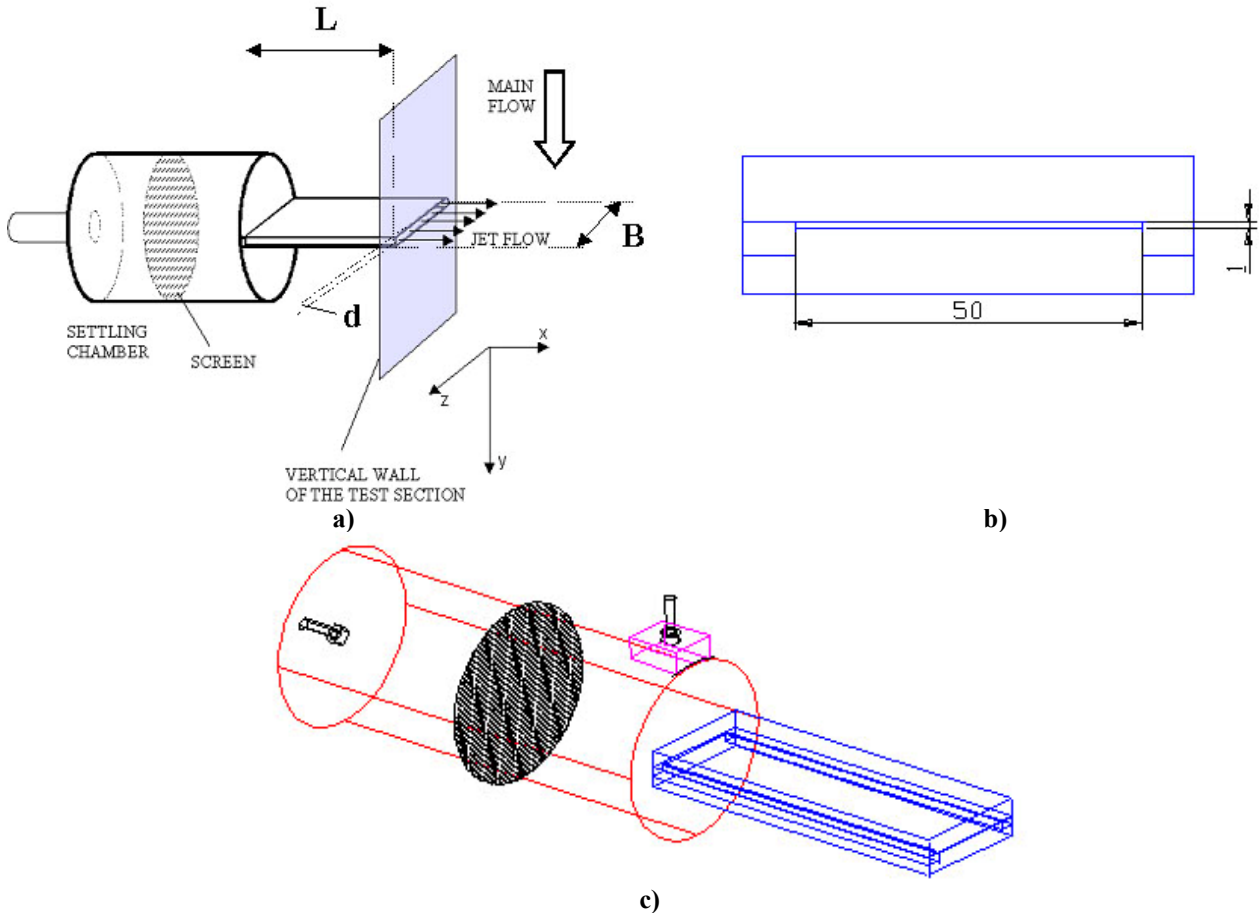


**Fig. 3:** Planar jet duct and its settling chamber: a) planar jet mounted in the middle of the test section; b) transversal section ( $B \times d$ ); c) three-dimensional view of the planar jet.

This set up was adopted in the visualizations and PIV measurements.

Two types of flow visualization were carried out. In the first case, visualizations were performed by mixing milk with the water within the tank which drives the jet. In the second case we have used tracer particles of lycopodium that have been illuminated via a laser light sheet produced by a continuous argon 150 mW laser source.

The PIV measurements were performed by using tracer particles seeding of lycopodium with a mean diameter of  $30\mu\text{m}$  that have been mixed with water.

Sequences of 480 images with a temporal distance between two consecutive images of  $1/30\text{s}$  were recorded using a digital commercial fotocamera Fujifilm FinePix S602 with resolution of  $640 \times 480$  pixels.

The velocity vector is evaluated in an interrogation window as the ratio between the averaged displacement of the particles and  $\Delta t$ . Particle displacement within an interrogation window is evaluated applying a cross-correlation technique based on two-dimensional discrete Fourier transform<sup>1</sup>. Interrogation windows size of  $64 \times 64$  pixels, 50% overlapped, is used for the evaluation

<sup>1</sup> The PIV software used in this work was the freeware *Matpiv 1.6* (<http://www.math.uio.no/~jks/matpiv/>) written by Prof. Johan Kristian Sveen (Dep. of mathematics, Mechanical division, Oslo University, Norway).

of the transversal recordings. Hence, the distance between two adjacent vectors in the physical space is around 0.5 cm. It has been used a “window offset” method to increase the signal-to-noise ratio and remove the displacement bias. At a first step, the displacement to integer accuracy is estimated and then the size of the interrogation window is halved.

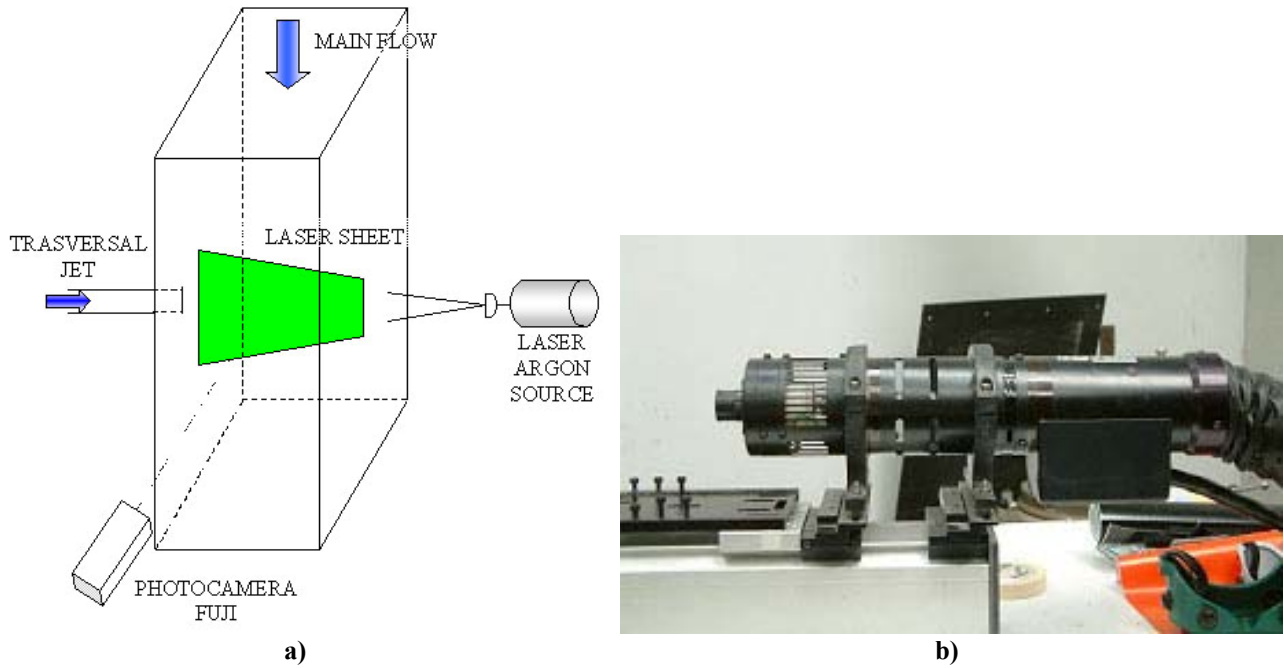


**Fig. 4:** PIV set-up (a) and continuous 150 mW argon laser source (b).

The flow conditions are characterized by means of three global non-dimensional parameters:

$$Re_j = \frac{U_j d}{\nu} \quad Re_\infty = \frac{U_\infty D}{\nu} \quad R = \frac{U_j}{U_\infty}$$

The free-stream velocity is varied in the range 1÷3 cm/s and the velocity ratio R is in the range 0.5÷12 (Tab. 1).

$U_j$ (cm/s)	$Re_j$	$Q_\infty$ (l/h)	$U_\infty$ (cm/s)	$Re_\infty$	$R$
0.5 ÷ 20	5 ÷ 200	360 ÷ 1080	1 ÷ 3	1000 ÷ 3000	0.5 ÷ 12

**Tab. 1:** Test cases analyzed in our experiments

The quality of the main stream as been quantified in terms of flow uniformity, turbulence levels and boundary layer thickness. The flow uniformity and turbulence levels at  $U_\infty=1\text{cm/s}$  have been evaluated by the spatial standard deviation  $\sigma_s$  and the temporal Relative Turbulence Level (RTL) using a number of samples of the order of 480. These values are  $\sigma_s=0.0086\text{ cm/s}$  and  $\text{RTL}=0.055$ . The boundary layer on the wall of the test section is laminar and stationary and its thickness is  $\delta=2.5\text{cm}$ . The corresponding displacement thickness is  $\delta^*=0.6651\text{cm}$ .

### 3. Results

The effect of the velocity ratio  $R$  is first analysed from a global viewpoint by the study of the jet axis curvature variation (Fig. 5). This effect is studied taking advantage of stream-lines obtained by the analysis of the PIV velocity fields (see e.g. Fig. 6). An increase of  $R$  leads to a decrease of bending with a lower curvature of the jet axis (Fig. 7).

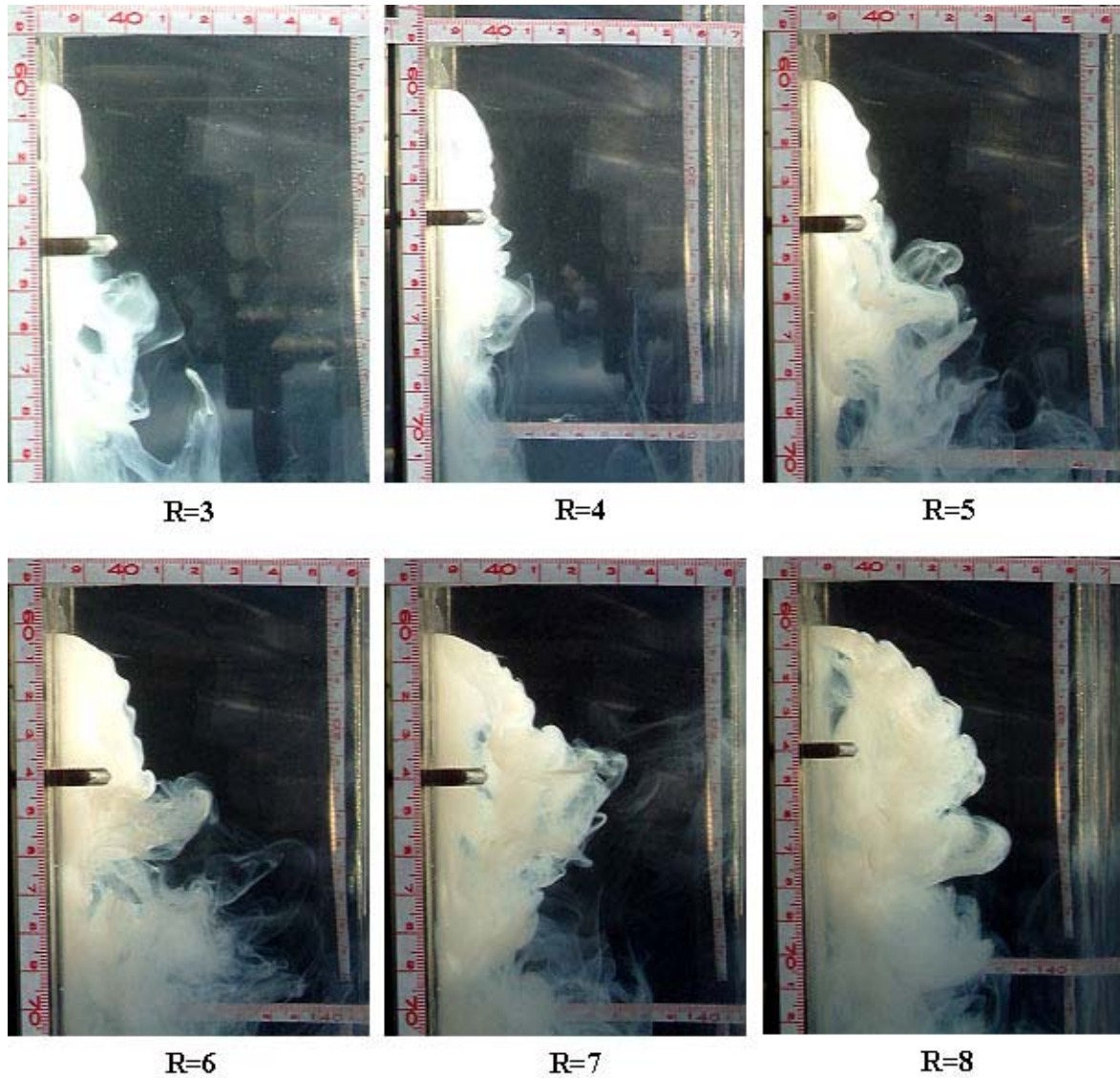


**Fig. 5:** Flow visualization in the range  $R=3\div 8$ .

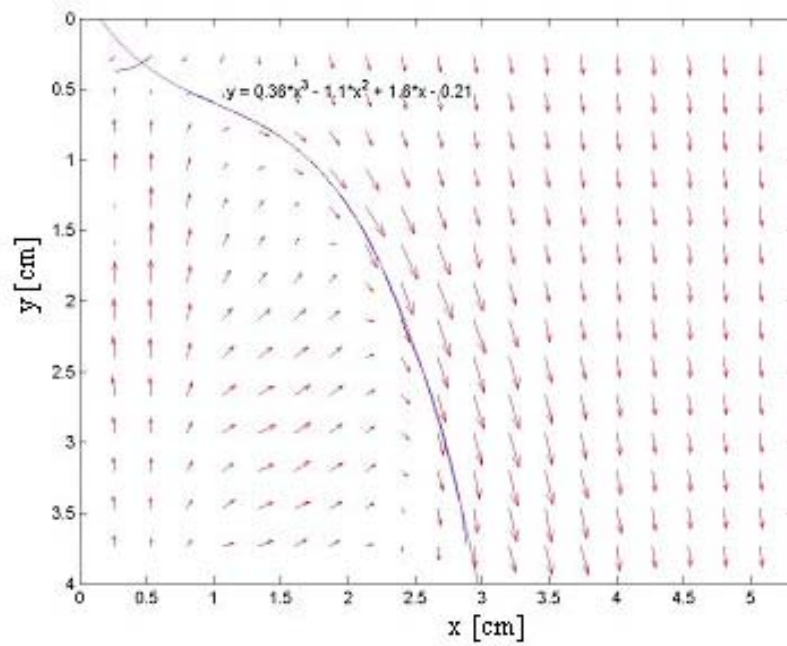


**Fig. 6:** PIV averaged velocity field and jet stream-lines (trajectory) originating from the jet exit at  $R=6$

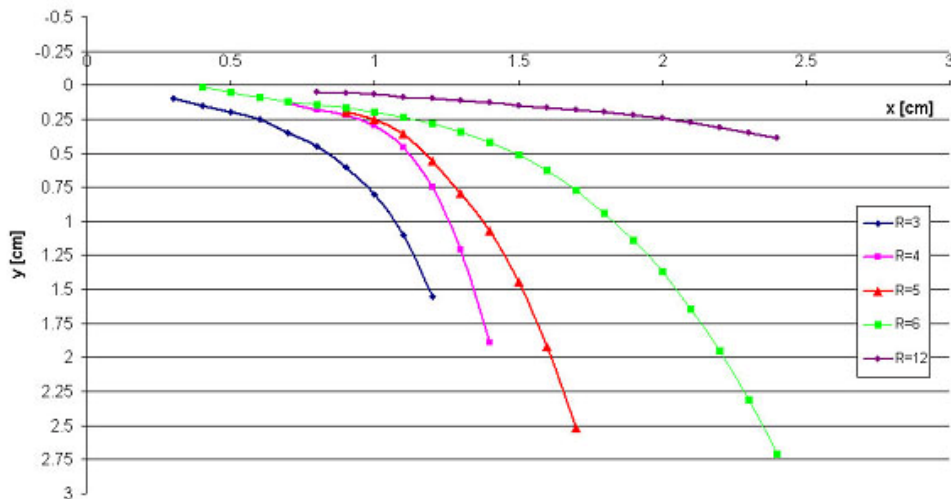


**Fig. 7:** Jet trajectory as functions of the velocity ratio  $R$  in the range  $R=3 \div 12$ .

The variation of  $R$  significantly affects the evolution of vortical structures and the interactions among them. We can note the presence of different flow regimes characterized by destabilization mechanisms governed by  $R$  and showing significant differences with respect to the instability behaviours expected for free jets.

At low  $R$  ( $R < 3$ ) the jet flow is not able to cross the boundary layer and it is close to the wall without any instability structures.

At  $R=3$  (Fig. 8) we note some instabilities along the shear layer and the regular formation of some vortical structures that are carried downstream by the main flow. As shown in Fig. 9 and Fig. 10 the vortical structures are in the lower side of the shear-layer and they present a clockwise vorticity (red colour in Fig. 10). The regular structures release of shear layer wake-like vortices at a frequency  $f=0.33\text{Hz}$  and a characteristic Strouhal number (defined as  $St=fd/U_j$ )  $St=0.011$ .



**Fig. 8:** Longitudinal flow visualization of the planar jet mixed with lycopodium at  $R=3$ ,  $Re_j=30$ ,  $U_\infty=1$  cm/s ( $f=0.33$  Hz,  $St=0.011$ ).

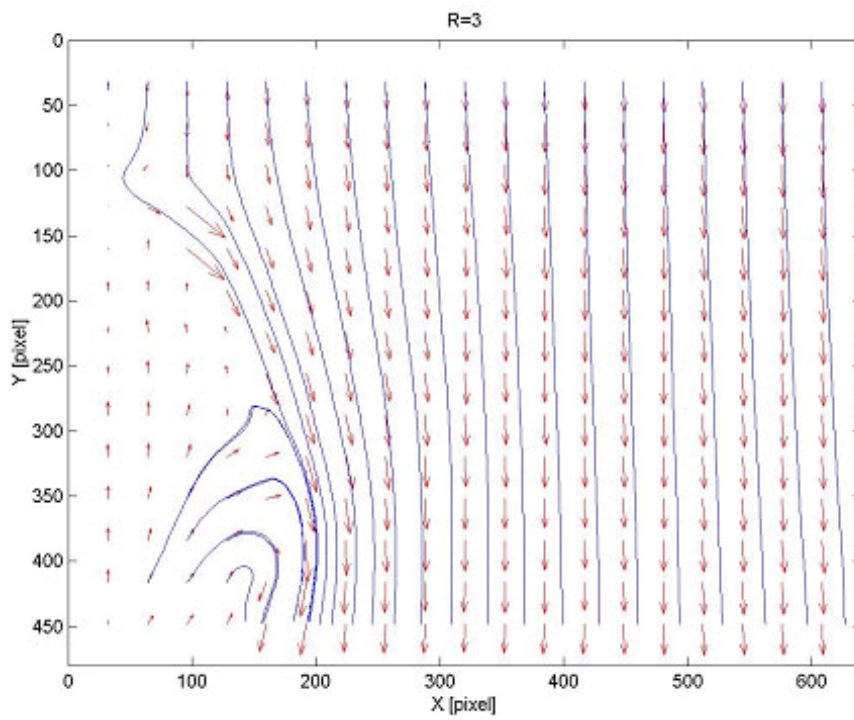


**Fig. 9:** PIV instantaneous velocity field and stream-lines at  $R=3$ .

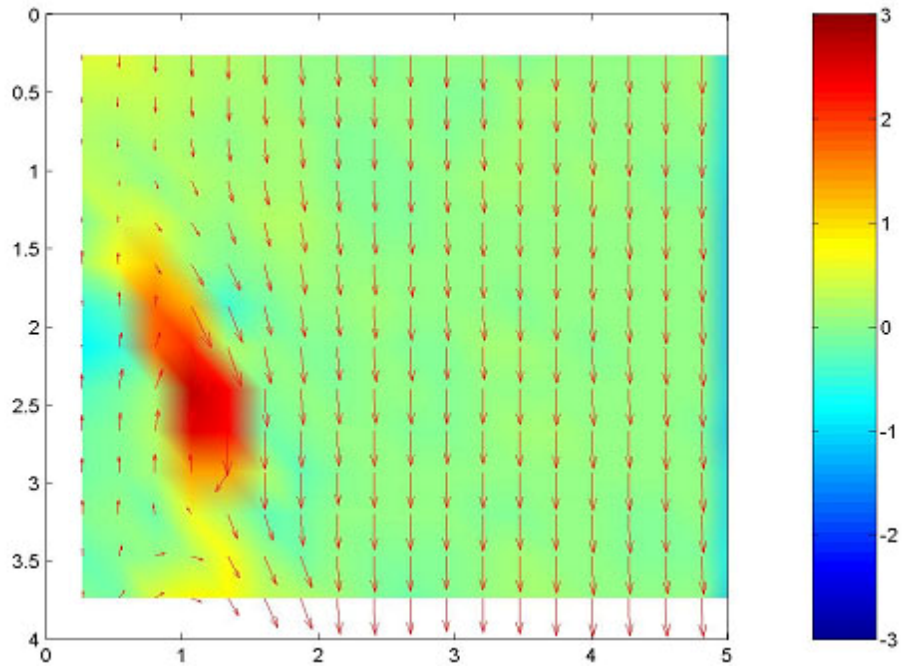


**Fig. 10:** Contour plot of an instantaneous velocity and vorticity field amplitude at  $Re=3$ .

In the range  $3 < R < 6$  (Fig. 11) the shear-layer of the planar jet has large fluctuations and its instability seems to be driven by the action of the cross-stream leading to the formation of wake-like vorticity dominated structures.

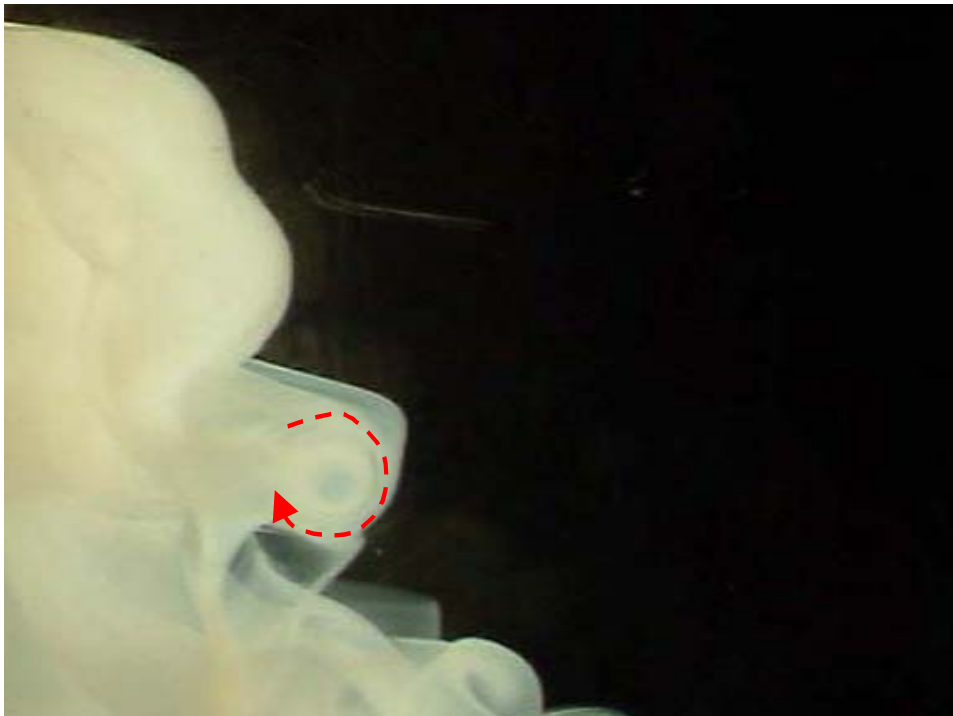


**Fig. 11:** Longitudinal flow visualizations of the planar jet at  $R=5$

The change of the flow behaviour occurs at  $R=6$  (Fig. 12) that represents the transitional value, in fact the jet flapping lead to the formation of SLV structures with opposite sign in the upper side of

the shear layer. The Kelvin Helmholtz instability mechanisms proper of mixing layers seems to prevail and at  $R > 6$  jet-like SLV are observed. In fact these SLV jet-like structures present a counter clockwise vorticity (blue colour in Fig. 14) and they have a magnitude with the same order of the lower SLV wake-like structures in this configuration. As shown in Fig. 13 the lower and the upper structures are ever coupled with a pairing phenomenon often seen in free jets. The vortices are released with a frequency  $f = 2.73$  Hz and  $St = 0.045$  confirming a different regime with respect to  $R < 6$ .

Our experiments have been mainly conducted with  $U_\infty = 1$  cm/s ( $R = 6$ ) and the jet Reynolds number for this transitional value is  $Re_j = 60$  corresponding to the value observed by Sato [4] for the transitional condition to turbulent regime in the free planar jet case.

Others experiments at the same  $Re_j$  but at different  $U_\infty$  (and hence  $R$ , e.g.  $U_\infty = 1$  cm/s and  $R = 3$ ) seem to show that the driving parameter for the formation of SLV structures with a counter clockwise vorticity seems not to be  $Re_j$  rather than  $R$ .

For  $R > 6$  (Fig. 15) up to  $R$  approximately 10 we can observe the two type of SLV like the case  $R = 6$ . This behaviour gets to the free planar jet dynamic at larger  $R$  than 10.

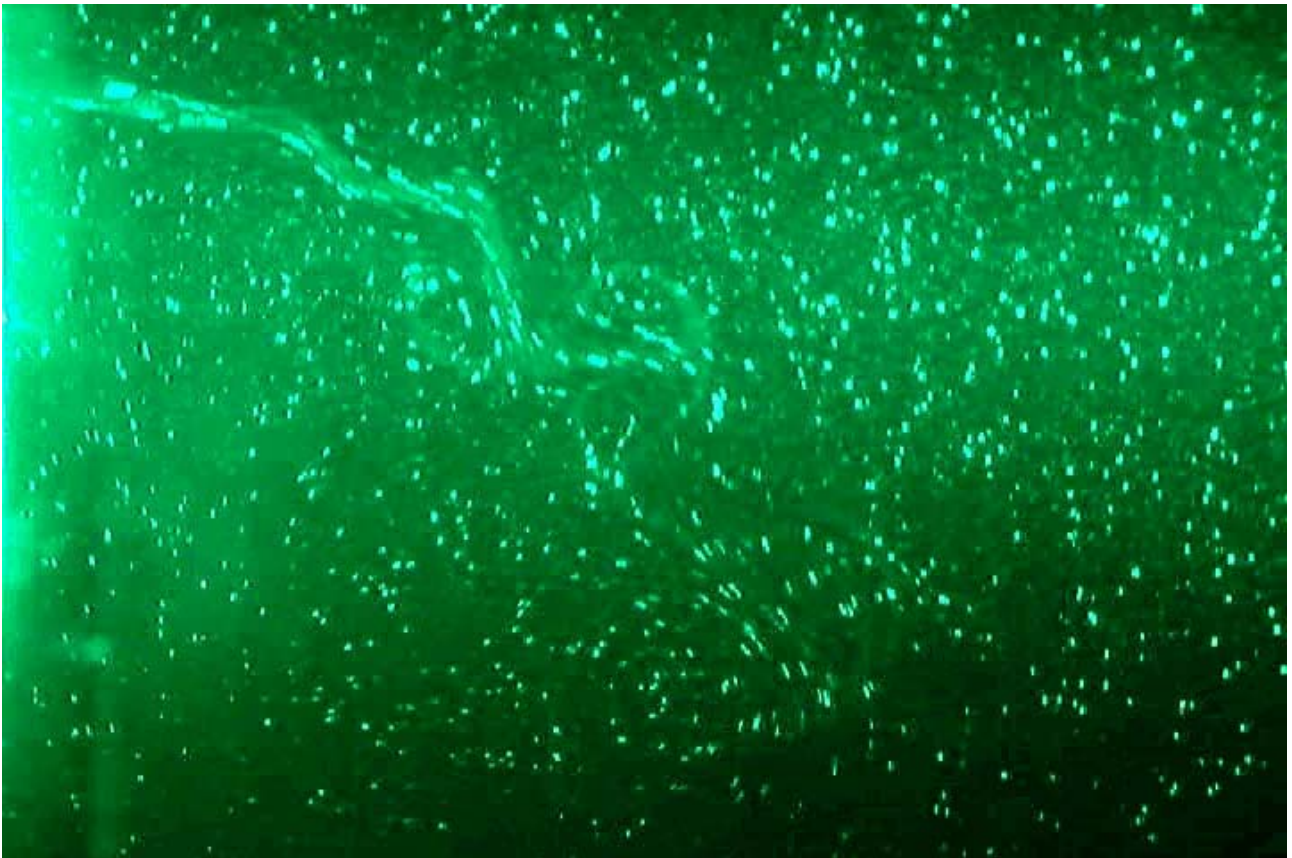


**Fig. 12:** Longitudinal flow visualization of the planar jet mixed with lycopodium at  $R = 6$ ,  $U_\infty = 1$  cm/s ( $f = 2.73$  Hz,  $St = 0.045$ ).

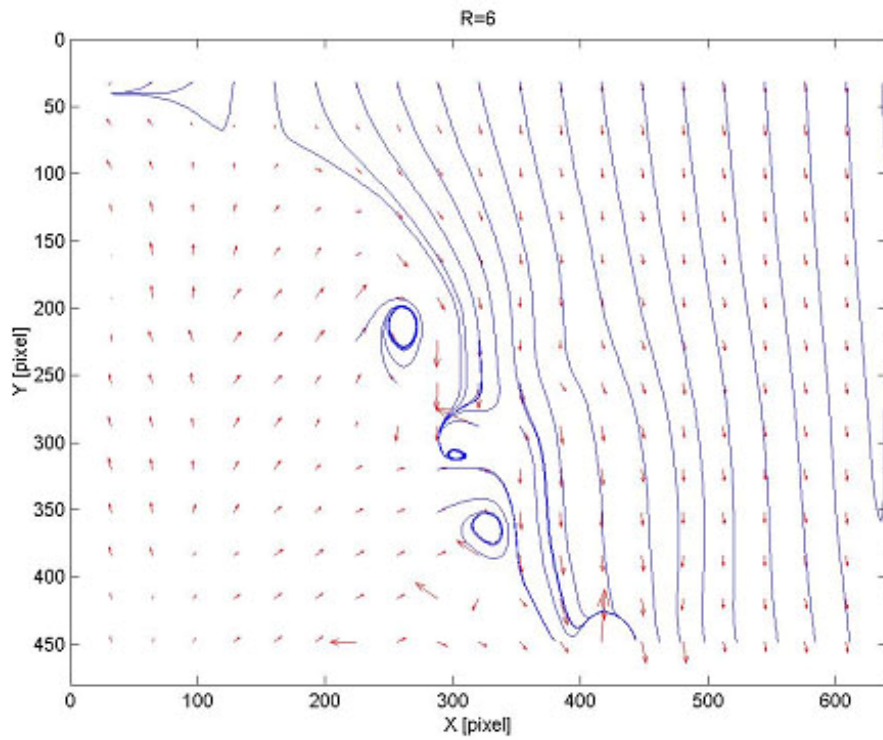


**Fig. 13:** PIV instantaneous velocity field and stream-lines for  $R=6$ .

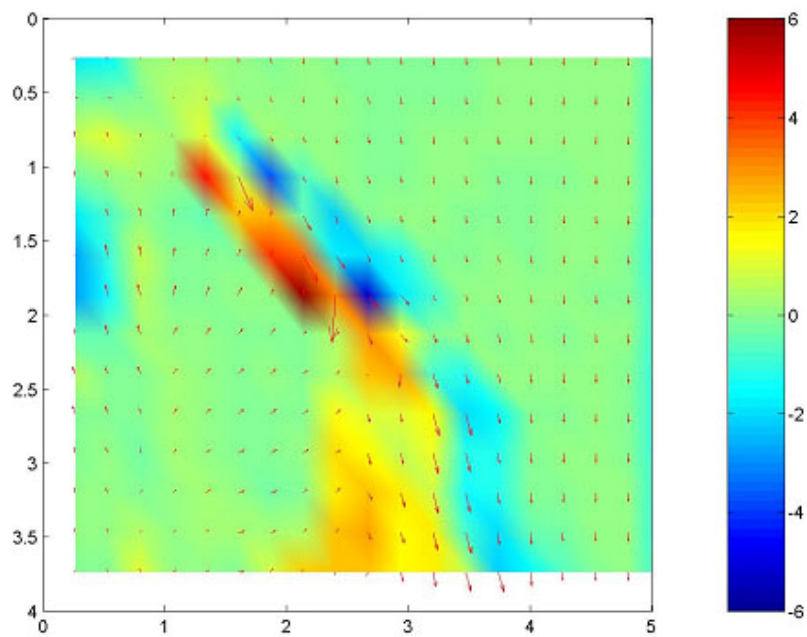


**Fig. 14:** Contour plot of an instantaneous velocity and vorticity field amplitude at  $Re=6$ .



**Fig. 15:** Longitudinal flow visualizations of the planar jet at  $R=9$

The shear layer vortical structures above observed in the longitudinal view have a horseshoe shape in the frontal view at the same way of the free planar jets [6]. As shown in Fig. 16a-b these vortical structures are very weak at  $R < 6$  with an clockwise vorticity on the edge and they are quickly destroyed at a distance of about 1.5cm from the exit jet. The SLV jet-like structures at  $R \geq 6$  (Fig. 16c-d) are stronger and more stable as they exist up to a distance of about 3.5cm from the exit jet; their destruction starts with the formation of secondary instabilities (Fig. 16d) that come out from the edge of the horseshoe shear layer vortices.

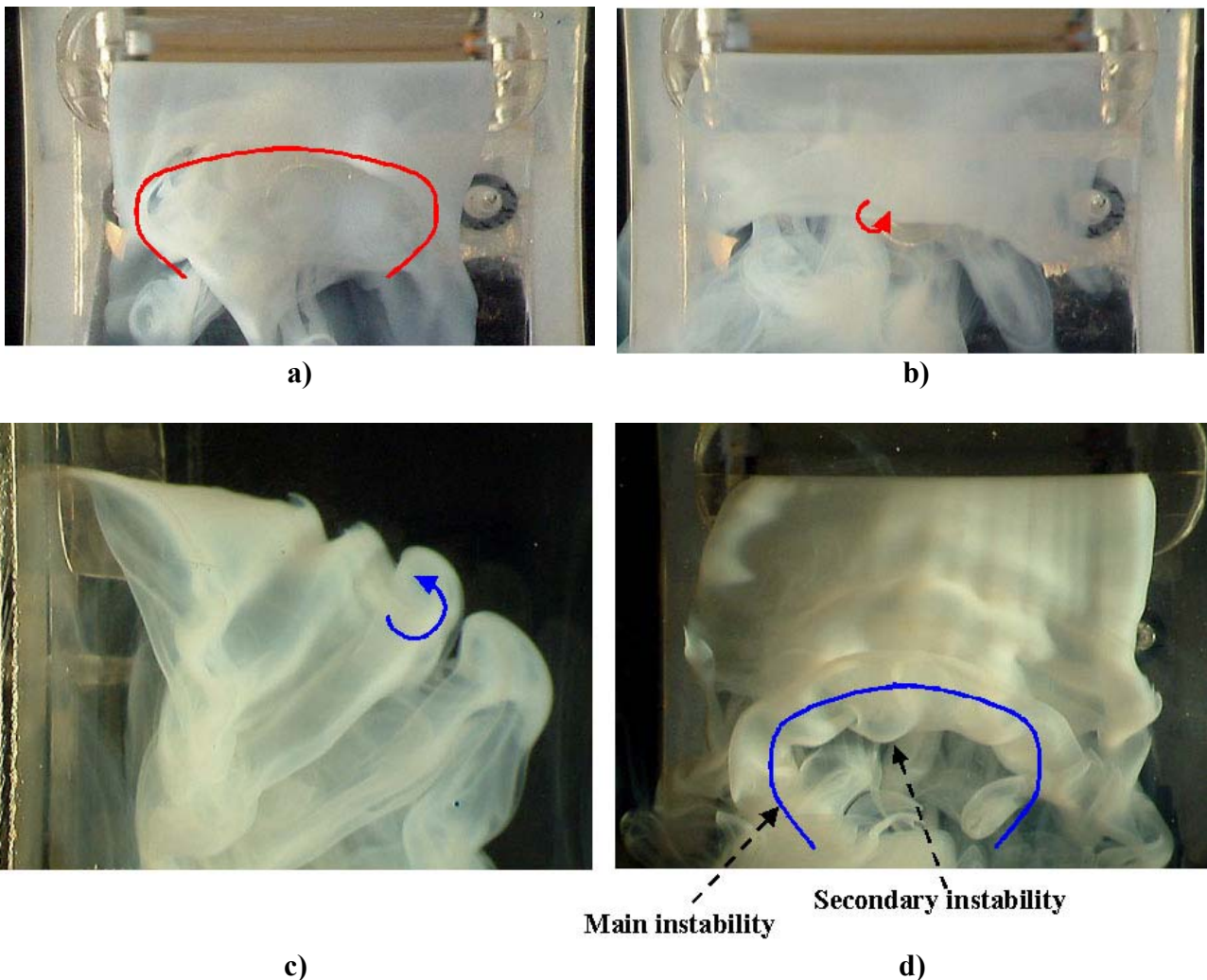


**Fig. 16:** Shear layer vortices at different conditions:  
a) frontal view at  $R=4$ ; b) frontal view at  $R=4.5$ ; c) longitudinal view at  $R=6$ ; d) frontal view at  $R=6$

## 4. Conclusions

A planar jet at low Reynolds numbers issuing in a cross flow is studied in order to analyze the SLV dynamics with no influence of the CRVP. It has been analyzed experimentally by flow visualizations and quantitative PIV measurements. The main physical results achieved are summarized as follows.

The planar jet presents distinct flow regimes whose characteristics depend on the  $R$  magnitude.

At low  $R$  ( $R < 3$ ) the jet flow is close to the wall without any instability structures. At  $R = 3$  we note some instabilities along the shear layer and the regular formation of some vortical structures that are in the lower side of the shear-layer and they present a clockwise vorticity. In the range  $3 < R < 6$  the shear-layer of the planar jet has large fluctuations and its instability seems to be driven by the action of the cross-stream leading to the formation of wake-like vorticity dominated structures. At  $R = 6$  the jet flapping lead to the formation of SLV structures with opposite sign in the upper side of the shear layer (jet-like structures). For  $R > 6$  up to  $R \cong 10$  we can observe the two type of SLV like the case  $R = 6$ . This behaviour gets to the free planar jet dynamic at larger  $R$  than 10.

The shear layer vortical structures observed have a horseshoe shape in the frontal view. These vortical structures are very weak at  $R < 6$  with a clockwise vorticity on the edge and at  $R \geq 6$  they are stronger and more stable with opposite vorticity.

The destabilization of the shear layer in the planar jet in cross-flow is leaded by SLV because there are not CRVP. It happens in similar way to circular jets, in fact the planar jet such as the circular jet presents two principal distinct flow regimes. This transitional value that was  $R \cong 3$  for circular jet configuration [2] now is  $R \cong 6$  (corresponding to  $Re_j = 60$ ) for planar jet configuration. Hence this destabilization seems leaded by RLV rather than CRVP for the circular jets in cross-flow too.

The obtained results seem to suggest the possibility of improving mixing in cross-flow configurations by controlling only by RLV and not CRVP.

## References

1. Kelso R.M., Lim T.T. and Perry A. E. An experimental study of round jets in cross flow. *J. Fluid Mech.*, Vol. 306, pp. 111-144, 1996.
2. Camussi R., Guj G. and Stella A. Experimental study of a jet in cross flow at very low Reynolds number. *J. Fluid Mech.*, Vol. 454, pp. 113-144, 2002.
3. Mikhail R., Chu V. and Savage S.B. The reattachment of a two dimensional turbulent jet in a confined cross flow. *Proc IAHR Congress*, San Paulo, Brazil, Vol. 3, pp. 414-415, 1975.
4. Sato H., The stability and transition of a two-dimensional jet, *J. Fluid Mech.* Vol. 7, pp. 53-83, 1960.
5. Sato H. and Sakao F., An experimental investigation of the instability of a two-dimensional jet at low Reynolds numbers, *J. Fluid Mech.*, Vol. 20, part 2, pp. 337-352, 1964.
6. Lo S.H., Voke P.R., Rocloff N.J., Three dimensional vortices of a spatially developing plane jet, *International Journal of Fluid Dynamics*, Vol. 4, article 1, 2000.